doi: 10.22564/rbgf.v13i1.1176

OBSERVATIONS OF ATMOSPHERIC DENSITY AND TEMPERATURE BETWEEN 35 AND 70 KM BY RAYLEIGH LIDAR AT SÃO JOSÉ DOS CAMPOS, SP

P. P. Batista, B. R. Clemesha & D. M. Simonich

During 1993, a total of 34 nigths of measurements of the Rayleigh backscattered signal was obtained at São José dos Campos, SP, (23° S, 46° W), with a laser radar (lidar). Relative atmospheric density and absolute temperature profiles between 35 and 70 km of height were determined. The performance of the lidar system was evaluated on the basis of the number of laser shots necessary to attain a certain accuracy. Measured temperature profiles show a consistently colder stratosphere and a hotter mesosphere compared with available models.

Key words: Rayleigh lidar; Rayleigh scattering; Lidar; Middle atmosphere; Atmospheric density; Atmospheric temperature.

OBSERVAÇÕES DA DENSIDADE E TEMPERATURA ATMOSFÉRICA ENTRE 35 E 70 KM POR UM LIDAR RAYLEIGH EM SÃO JOSÉ DOS CAMPOS, SP. *Durante 1993, um total de 34 noites de medidas do sinal Rayleigh retroespalhado foi obtido em São José dos Campos, SP, com um radar de laser (lidar). Perfis de densidades relativas e temperaturas absolutas da atmosfera entre 35 e 70 km de altura foram determinados. O desempenho do sistema de radar foi avaliado com base no número de disparos necessários para atingir determinada precisão. Os perfis medidos de temperatura mostram consistentemente uma estratosfera mais fria e mesosfera mais quente que os modelos disponíveis.*

Palavras-chave: *Lidar Rayleigh; Espalhamento Rayleigh; Lidar; Média atmosfera; Densidade atmosférica; Temperatura atmosférica.*

Instituto Nacional de Pesquisas Espaciais - INPE,
C. P. 515, 12201-970, São José dos Campos, SP, Brasil.

INTRODUCTION

A laser radar has been operated at São José dos Campos, SP, (23° S, 46° W), since 1969 (Clemesha & Rodrigues, 1971). Since that time, taking advantage of the several ways light can be scattered by atmospheric species and different laser wavelengths available, the lidar has been used to measure mainly the distribution of aerosol particles in the stratosphere by Mie scattering and the concentration of sodium atoms in the upper mesosphere and lower thermosphere by resonant scattering (see for instance Clemesha & Simonich (1978), Simonich et al. (1979), Clemesha (1984)).

The scattering of light by atmospheric molecules, independently of their nature (Rayleigh scattering), naturally provided the simplest way the laser could be used for upper atmospheric research, yielding directly relative atmospheric density. Nonetheless, in order to reach mesospheric and lower thermospheric altitudes the lidar system has to have very high output, which could only be attained with very powerful lasers or large collecting areas. Powerful Q-switched ruby lasers were used in the seventies to study atmospheric density, including tides (Kent & Wright, 1970; Kent et al., 1972), but only above 70 km because the high transmitted power introduced discrepancies for lower heights attributed to saturation effects and to the presence of aerosols. The development of laser technology in the end of the seventies and beginning of the eighties has provided lasers with high energy per pulse and very high repetition rate. Using a Neodymium-Yag laser, atmospheric density and temperature between 30 and 80 km have been successfully obtained in France and used to study gravity and tidal waves in the stratosphere and mesosphere, and planetary waves and stratospheric warming events in the stratosphere (Hauchecorne & Chanin, 1980, 1982, 1983; Chanin & Hauchecorne, 1981; Hauchecorne et al., 1987; Gille et al., 1991). Additionally to these works, measurements of density and temperature by Rayleigh lidar have also been reported in the USA (Gardner et al., 1989a), Japan (Shibata et al., 1986), United Kingdom (Jenkins et al., 1987) and Italy (Adriani et al., 1991).

With the installation of a new commercial laser (CANDELA Model LFDL-20), with a 2-3 J energy output and a maximum repetition rate of 10 Hz, the INPE lidar was adapted to measure the atmospheric density between 35 to 80 km and the temperature between 35 to 70 km, beginning in April, 1993. In this paper we present the methodology used to obtain the atmospheric temperature and an evaluation of the possibilities for the lidar, and discuss the first results obtained from April to December, 1993.

INSTRUMENTATION

The basic parameters and geometry of the INPE lidar are essentially the same as has been described elsewhere (Simonich et al., 1978; Clemesha, 1984). Tab. 1 gives the main parameters for transmitter and receiver. As another improvement related to the previous measurements a new Multichannel Digital Analyser (MDA) was used. This is a 640 channel MDA which gives a height resolution of 250 m. The laser bandwidth was reduced to 0.1 nm by birefringent filter inside the cavity and a filter with 0.7 nm full width at half maximum (FWHM) was used at the receiver. In a few measurements the filters were centered on 588.8 nm, away from the sodium line, but later they were centered at 589.0 nm to also obtain the sodium signal. The lower atmosphere signal was counted by a low sensitivity photomultiplier and the upper atmosphere signal by a high sensitivity photomultiplier. In this way, unsaturated signals beginning from approximately 10 km could be recorded and used to observe the stratospheric aerosol layer. The sum of the signals from 500 to 2000 shots of the laser was accumulated and recorded on hard and floppy disks of a microcomputer for subsequent analysis.

Transmitter		Receiver	
Energy per pulse		Area	0.39 m^2
Pulse duration	2 μs	Bandwidth	700 pm
Repetition rate	10 s^{-1}	Beamwidth	0.4 mR
Bandwidth	0.1 nm		
Beamwidth	0.15 mR	Height Interval	0.25 km
Wavelength	589 nm	Efficiency	2.4%

Table 1 - Specifications for the lidar.

Tabela 1 *- Especificações para o radar de laser.*

METHOD OF ANALYSIS

Part of the light transmitted upwards to the atmosphere is backscattered and collected by the optical system and counted as photons by a photomultiplier tube (PMT). These photons are divided by height range so that light collected from time $t_i - \Delta t/2$ to $t_i + \Delta t/2$ comes from the heights between $h_i - \Delta h$ and $h_i + \Delta h$. The number of photons per kilometer per shot is given by the so called Lidar Equation (Kent et al., 1967);

$$C(h_i) = \rho(h_i)\, \beta\, K\, T^2 / h_i, \qquad (1)$$

where $C(h_i)$ is the number of photons detected from a height h_i per kilometer per shot, $\rho(h_i)$ is the density of scattering molecules at height h_i, β is the Rayleigh backscatter function per molecule, T is the total atmospheric transmission from the lidar to the height h_i and K is a lidar constant which depends on the counting system efficiency. Normally, below 30 km the Rayleigh backscatter function should be added to the Mie backscatter function. The existence of an unusual aerosol load due to the eruption of the volcano Pinatubo, in the Philippines in 1991 (e.g. McCormick & Veiga, 1992), has increased the height above which the Mie scattering is negligible to nearly 35 km, so for heights above that we consider that all the signal is produced by Rayleigh scattering. The variable and unknown factor KT^2 is canceled out by taking the signal at a reference height h_r where the atmospheric density does not vary so much and is known by model or by measurements. We use the reference level at around 40 km and a model density for our station obtained from many radiosonde profiles and extrapolated for higher heights. In this case we obtain:

$$\rho(h_i) = \frac{C(h_i)\rho(h_r)h_i^2}{C(h_r)h_r^2}, \qquad (2)$$

where $\rho(h_i)$ is the atmospheric density at the height h_i, $\rho(h_r)$ is the atmospheric density at the reference height h_r, $C(h_i)$ and $C(h_r)$ are the photocounts per kilometer per shot at the heights h_i and h_r, respectively. The relative uncertainty in the density profile is considered to be equal to the statistical standard error:

$$\frac{\delta\rho(h_i)}{\rho(h_i)} = \frac{(N(h_i)+N_b)^{1/2}}{N(h_i)}, \qquad (3)$$

where $\delta\rho(h_i)$ is the standard deviation of the atmospheric density, $N(h_i)$ is the absolute photon count at h_i, and N_b is the background noise. This background noise is determined by the average of the counts from 110 to 120 km, where the Rayleigh and sodium signal are expected to be zero.

For the temperature determination the hydrostatic balance equation and the ideal gas law are used (Shibata et al., 1986; Gardner et al., 1986b):

$$dP = -\rho g dh, \qquad (4)$$

$$P = \rho RT/M, \qquad (5)$$

where P is the pressure, g the acceleration due to gravity, R the universal gas constant, T the temperature and M the mean molecular weight for air.

Eliminating the pressure from the two equations above, the temperature is obtained as:

$$T(h_i) = \frac{T(h_l)\rho(h_l)}{\rho(h_i)} + \frac{M}{R}\int_{h_i}^{h_l} \frac{\rho(r)}{\rho(h_i)} g(r)dr. \qquad (6)$$

Note that temperature at any level i depends only on the ratio between the densities in two different levels and on the temperature in the upper level l. Since the temperature at the upper level is generally unknown, the accuracy of the measurement will depend on $T(h_l)$. But, since this temperature is multiplied by the ratio between the density at the upper level and the density at the calculated level, the contribution of the first term in the right hand side of Eq. (6) decreases very fast below the reference level so that the contribution of the first term becomes very low at about two atmospheric scale heights below h_l. This is illustrated in the Fig. 1, where the curves represent the first and second term of the right hand side of Eq.(6) and the resulting sum. Note that for heights much lower than the reference height the temperature determination is almost independent of the reference temperature.

DATA

The observations began on April 14, 1993, when 11000 shots of the laser were given from 19:24 to 23:59 LT. Tab. 2 shows the days when the data were taken, the number of shots, and the time intervals of the measurements. In Fig. 2 the density profile normalized by the MSISE-90 model (Hedin, 1991) is shown between 35 and 80 Km for the nights of 30.11.93 (a) and 22.07.93 (b). The MSISE-90 model fits the monthly mean models given by the CIRA-86 (Barnett & Corney, 1985) in selected latitudes and heights to analytical functions such that the models can be evaluated for different latitudes, heights and times throughout efficient numerical code. Therefore, this model represents a density model for 23° latitude for the corresponding day. Our measured density is normalized to the model density at 40 km. At this height the effect of the aerosols is believed to be very small. Values are

calculated at each kilometer using a moving average of 4 Km. The curves around the points correspond to ± 1 standard deviations calculated according Eq. (3). The maximum height that can be reached depends mainly on the number of shots given by the laser. We are using the criterion that the normalized density is evaluated up to the level where the accuracy in density is 5%. In the examples shown in Fig. 2 (a), for 36000 shots this accuracy is obtained at 71 km, and in Fig. 2 (b) for 101000 shots this accuracy is obtained at 80 km. High variability in the atmospheric density profiles caused by planetary, tidal and gravity wave propagation, is common at the stratosphere and mesosphere, as can be seen in the Figs. 2(a) and 2(b). In Figs. 3 (a) and 3(b), the corresponding temperature profiles calculated according to Eq. (6) are shown. The temperature at the upper level is also taken from the MSISE-90 model. The temperature accuracy is determined by error propagation formulas applied to Eq. (6) and a 15% error at 80 km is assumed. As explained above, at the higher levels, the error caused by the assumed temperature is very high, then the values of temperature are considered starting only ten kilometers below the higher density level. In Figs. 3(a) and 3(b) the dashed lines represent the model temperatures. Large deviation from the model is observed, especially, on the night of 22.07.93 when high mesospheric temperature is observed at around 65 km.

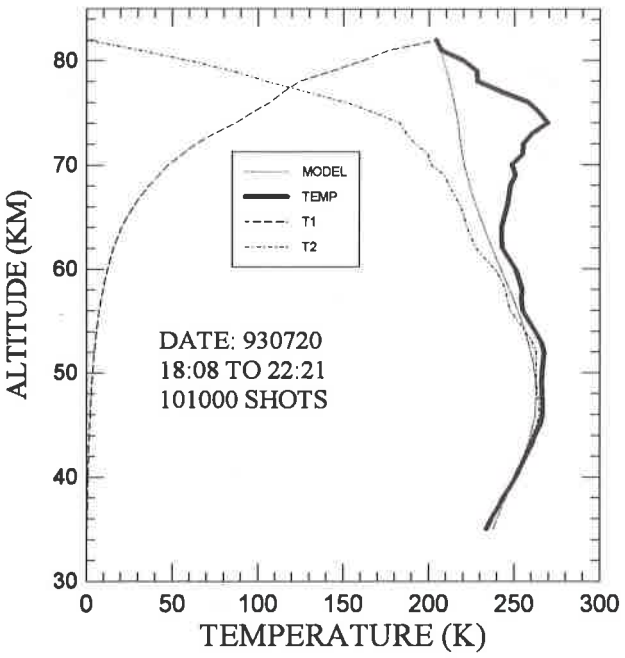

Figure 1 - Temperature determination according Eq. (6) for a selected night. First term (dashed curve), second term (dotted-dashed) and the sum (full line). Dotted line refers to the model.

Figura 1 - *Determinação da temperatura de acordo com a Eq. (6) para uma noite selecionada. O primeiro termo (curva tracejada), segundo termo (curva traço-ponto) e a soma das duas (linha cheia). A curva pontilhada refere-se ao modelo.*

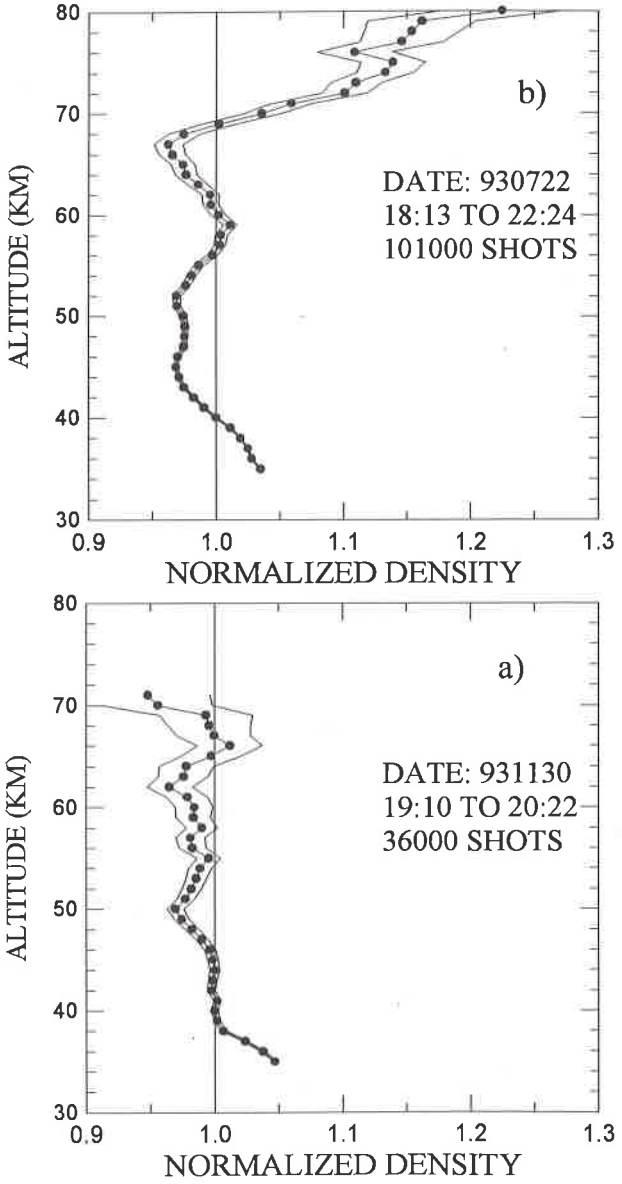

Figure 2 - Deviation of atmospheric density relative to the model for 30.11.93(a) and 22.07.93(b).

Figura 2 - *Desvio da densidade atmosférica relativo ao modelo para 30.11.93(a) e 22.07.93(b).*

Day #	Date DD. MM	# of Shots	Day of year	Start	Stop
1	14.04	11000	104	19:24	23:59
2	26.04	20300	116	19:14	21:09
3	27.04	4500	117	18:24	18:50
4	29.04	13500	119	18:14	20:15
5	30.04	5000	120	18:12	18:47
6	07.05	12000	127	18:07	19:08
7	11.05	7000	131	18:13	18:35
8	18.05	49500	138	18:00	01:13
9	19.05	46000	139	18:07	19:46
10	14.06	60000	165	18:19	04:29
11	15.06	10000	166	17:56	19:31
12	21.06	18000	172	17:46	21:00
13	22.06	23000	173	18:46	19:52
14	23.06	65000	175	17:53	04:49
15	30.06	30000	181	17:54	22:54
16	02.07	38000	183	22:39	04:59
17	05.07	84000	186	18:27	21:54
18	20.07	101000	201	18:08	22:21
19	22.07	101000	203	18:13	22:24
20	02.08	100000	214	18:13	22:13
21	20.08	93000	232	18:12	22:16
22	26.08	101000	238	18:24	22:34
23	30.08	102000	242	18:30	22:41
24	06.09	60000	249	18:26	20:55
25	13.09	69600	259	19:19	22:26
26	07.10	36000	280	19:23	21:21
27	08.10	88000	281	18:41	21:33
28	20.10	36000	293	19:20	21:20
29	29.10	78000	302	19:25	22:34
30	11.11	20000	315	18:49	19:24
31	12.11	40000	316	20:16	22:52
32	27.11	62000	331	19:13	21:14
33	30.11	36000	334	19:10	20:22
34	13.12	30000	347	22:12	23:13

Table 2. Rayleigh lidar data for 1993.

Tabela 2 *- Dados do radar de laser Rayleigh para 1993.*

The density and temperature accuracies for 36000 and 101000 shots as a function of altitude are shown in Figs. 4(a) and 4(b), respectively. It is noted that a density accuracy of less than 0.1% can be obtained at 40 km, but around 100000 shots of the laser are necessary to obtain a 5% accuracy at 80 km

For the temperature an accuracy of 1 K can be obtained at around 60 km, but in order to obtain an accuracy better than 10 K at around 70 km, more than 100000 shots are necessary. In Fig. 5 the number of shots necessary to obtain a 5% accuracy is shown as a function of the height where this occurs. All the data analyzed here are plotted in the figure. The scattering of the data points is due to the variation of the transmitted power, system alignment and the atmospheric transmission on different days. The straight line shown in the figure is the least mean square fit to the data points. From this fit it is shown that the number of shots should be doubled in order to obtain a 5 km increase in the maximum height. On the right scale the time required to give the corresponding number of shots is shown. For this correspondence, the maximum repetition rate of the laser is assumed (10 pps) and a maximum of 2000 shots are accumulated and recorded on floppy and hard disks. Taking into account the recording and processing time these 2000 shots take 4 min to be acquired. The previous analysis can be to used to define the limits of our lidar system in studying different atmospheric phenomena. The capability of the system for gravity wave studies is very limited since a minimum of 10 minutes of measurements would be necessary to accumulate shots to obtain each density

profile and the altitude would be restricted to below ≈60 km. For tidal studies, hourly profiles would be enough and in this case about 30000 shots could be given obtaining densities up to 75 km and temperatures up to 65 km. The restriction in this case is the high number of shots necessary to cover an entire night, 3.6×10^5 shots. One dye load is enough to about 50000 shots, thus the system should be cleaned and the dye changed about seven times during the night. These considerations show that the system can be easily used for studies of long-term variations of the atmospheric densities and temperatures and variations in a sequence of days, and with some difficulties, for tides and long-period gravity waves..

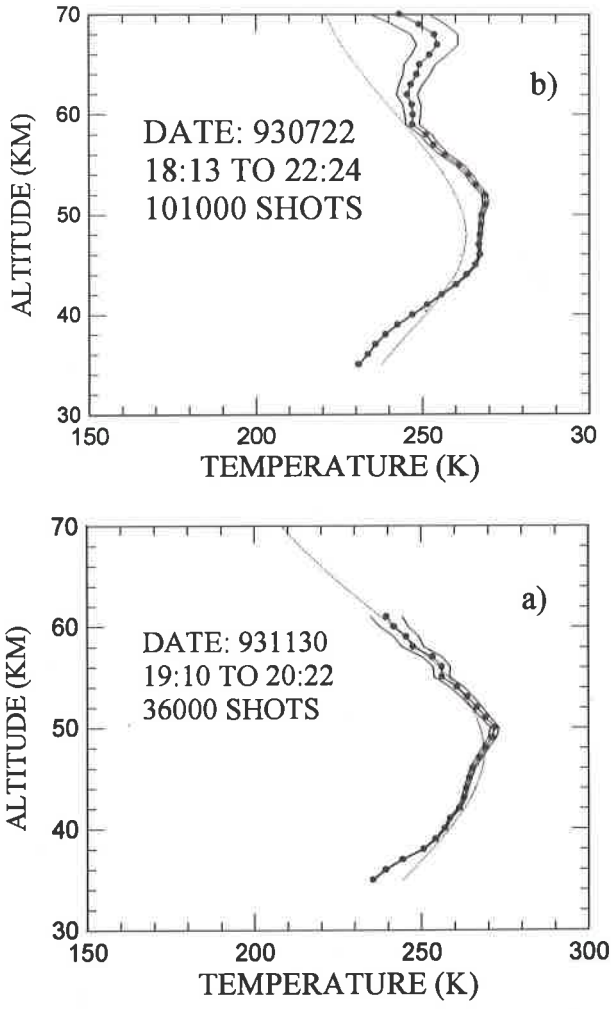

Figure 3 - Atmospheric temperatures for 30.11.93(a) and 22.07.93(b). Dotted lines refer to the MSISE-90 model.

Figura 3 *- Temperaturas atmosféricas para 30.11.93(a) e 22.07.93(b). Linhas pontilhadas se referem ao modelo MSISE-90.*

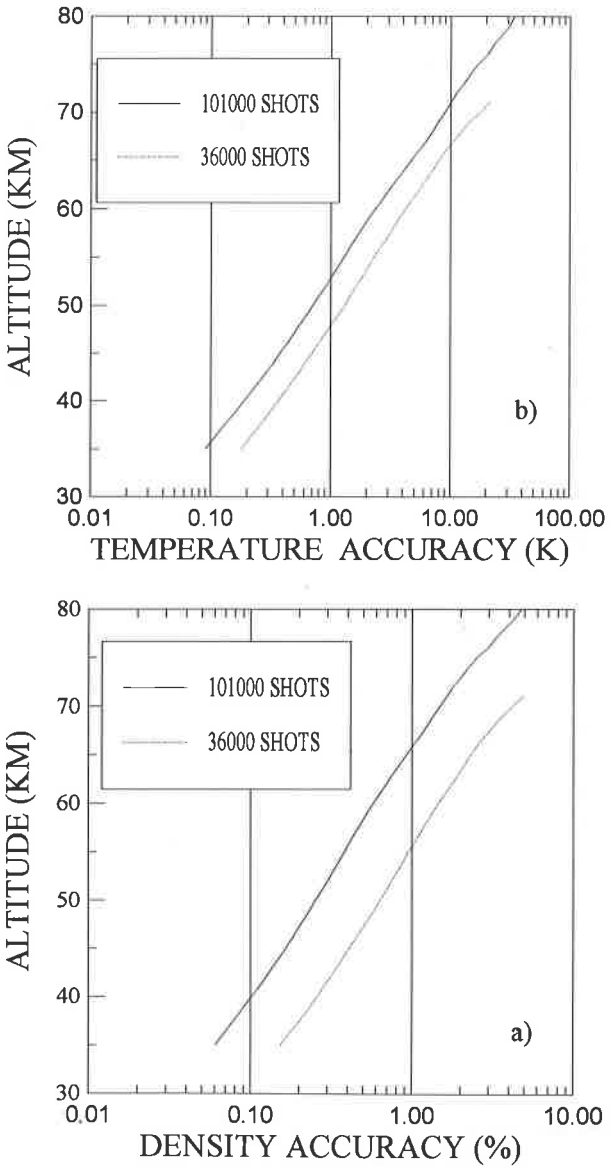

Figure 4 - Density and temperatures accuracies ((a) and (b)) for 101000 shots (full line) and 36000 shots (dotted line).

Figura 4 *- Precisão nas medidas da densidade e temperatura ((a) e (b)) para 101000 disparos do laser (linhas cheias) e 36000 disparos (linhas pontilhadas).*

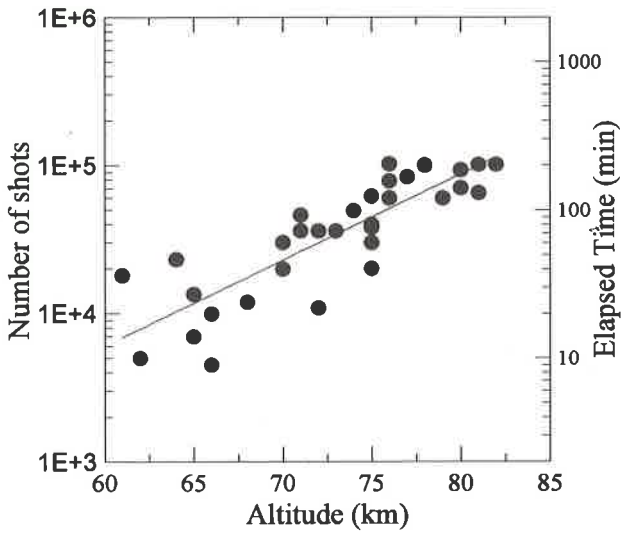

Figure 5 - Number of shots and total time necessary to obtain a 5% accuracy as a function of height.

Figura 5 *- Número de disparos e tempo total necessário para obter precisão de 5% em função da altura.*

The capability of the system having been defined, we started to measure the Rayleigh profiles on a regular basis, taking at least one measurement per week, whenever good weather conditions existed. Unfortunately, one of the high-voltage capacitors used in the laser broke down on 13.12.93, and it was not possible to obtain a replacement until April 94, so a complete year of measurements could not be obtained for the definition of the annual cycle. Time-height contour plots for the observed temperatures between 14.04.93 and 13.12.93 are shown in Fig. 6(a). Temperatures are contoured at each 5 K and missing data are indicated by blank areas. In Fig. 6(b) similar contour plots are shown for the MSISE-90 model and in Fig. 6(c) the difference between the data and the model. As can be noted, substantial and consistent differences exist between the observed data and the model. In the upper stratosphere over São José dos Campos temperature is consistently lower than the model by an amount that can be more than 5 K. At the stratopause the temperature exceeds the model by nearly 5 K and this difference becomes larger, exceeding 10 K, at upper levels

The detected higher mesospheric and lower stratospheric temperatures seems to be in a different sense than the temperature trend measured at the 55 km level by the French Rayleigh lidar at Haute Provence (44^0 N) from 1979 to 1990 (Aikin et al., 1991). In that work a long-term decrease of the mesospheric temperature is reported, which is attributed to the increase of the amount of longwave radiation emission which cools the mesosphere, caused by the increases in

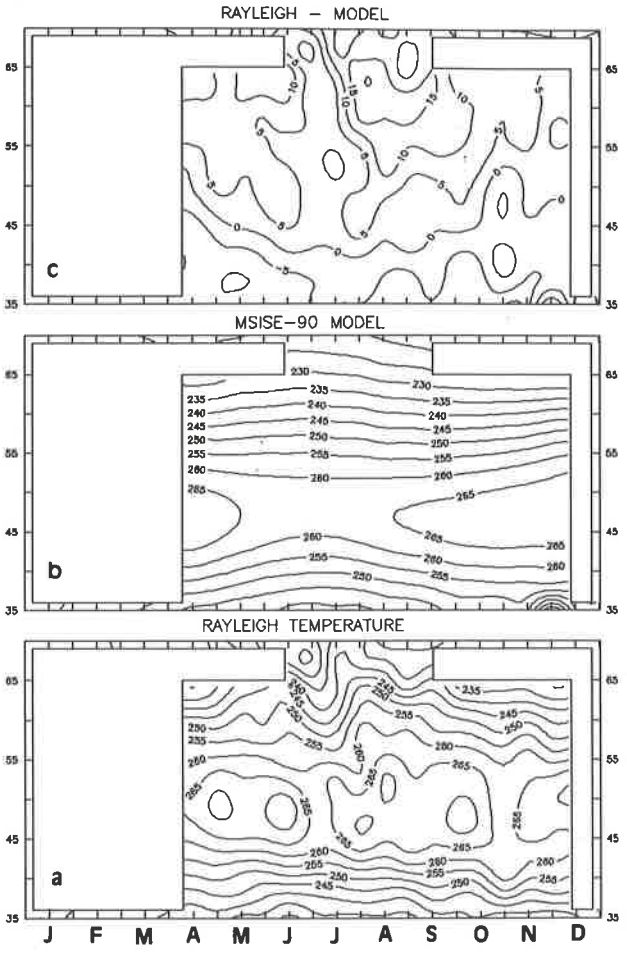

Figure 6 - Contour plots for the temperature in K: (a) Measured by Rayleigh lidar; (b) given by MSISE-90 model; and (c) the difference between data and model.

Figura 6 *- Contornos de temperatura em K: (a) Medidas pelo lidar Rayleigh: (b) dadas pelo modelo MSISE-90: e (c) a diferença entre dados e modelo.*

gases of anthropogenic origin such as CO_2. However, in a recent report by the same group (Keckhut et al., 1994), an anomaly in the temperature climatology is detected. The linear decrease of temperature at mesospheric altitudes was interrupted after 1992, following the injection of aerosols in the stratosphere by Pinatubo. The anomaly is reported as continuing in 1993, during the decreasing phase of the aerosol layer. The authors suggest that the warming in the lower stratosphere caused by the aerosol layer induced perturbations in the whole middle atmosphere. Unfortunately, we do not have data for the period before 1993, but it could be that the temperature structure of the middle atmosphere was indeed perturbed during this year.

CONCLUSIONS

Measurements of atmospheric densities and temperatures in the upper stratosphere and mesosphere by means of a Rayleigh lidar in São José dos Campos over a period of eight months in 1993 have been presented. An analysis of the system performance has shown that the system is very adequate for long-term density and temperature variations and with little difficulty can also be used for tidal and gravity wave studies. The study of average temperature profiles from April to December has shown a colder stratosphere and hotter mesosphere as compared with the MSISE model. Since atmospheric models for this atmospheric region are based mainly on rocket measurements, with scarce coverage at low and equatorial latitudes, and on satellite measurements with poor height resolution, lidar measurements can be used for satellite validation purposes and to improve models as well as for long-term studies of temperature and density at middle atmosphere. Measurements on a regular basis will continue in the future in order to cover several annual cycles and in special campaigns for wave propagation studies.

ACKNOWLEDGEMENTS

We are grateful to Rubens Carlos de Oliveira for his assistance in system operation and data collection. Thanks are also due to Fundação de Amparo à Pesquisa do Estado de São Paulo (FAPESP) for support through grant 93/1221-5.

REFERENCES

ADRIANI, A., GOBBI, G. P., CONGEDUTI, F. & Di DONFRANCESCO, G. - 1991 - Lidar observations of stratospheric temperature: November 1988-November 1989. Ann. Geophysicae, **9**: 252-258.

AIKIN, A. C., CHANIN, M. L., NASH, J. & KENDING, D. J. - 1991 - Temperature trends in the Lower Mesosphere. Geophys. Res. Lett., **18**:416-419.

BARNETT, J. J., & CORNEY, M. - 1985 - Middle atmosphere reference model derived from satellite data. Handb. MAP, **16**, Edited by Labitzke, K., Barnett, J. J. & Edwards, B. pp. 47-85, Sci. Comm. for Sol. Terr. Phys. Secr. Univ. of Ill., Urbana.

CHANIN, M. L. & HAUCHECORNE, A. - 1981 - Lidar observations of gravity and tidal waves in the Stratosphere and Mesosphere. J. Geophys. Res., **86**: 9715-9721.

CLEMESHA, B. R. - 1984 - Lidar studies of alkali metals. Handbook of MAP, **13**:99-112.

CLEMESHA, B. R. & RODRIGUES, S. N. - 1971 - The stratospheric scattering profile at 23° S. J. Atmos. Terr. Phys., **33**: 1119-1123.

CLEMESHA, B. R. & SIMONICH, D. M. - 1978 - Stratospheric dust measurements 1970 - 1977. J. Geophys. Res., **83**: 2403-2408.

GARDNER, C. S., MILLER, M. S. & LIU., C. H. - 1989a - Rayleigh Lidar observations of gravity wave activity in the Upper Stratosphere at Urbana, Illinois. J. Atmos. Sci., **46**: 1838-1854.

GARDNER, C. S., SENFT, D. C., BEATTY, T. J., BILLS, R. E. & SEGAL, A. C. - 1989b - Rayleigh and sodium lidar techniques for measuring middle atmospheric density, temperature and wind perturbations and their spectra. In World Ionosphere/Thermosphere Study Handbook, 2, edited by Liu, C. H. & Edwards, B. International Congress of Scientific Unions, Urbana: 148-187.

GILLE, S. T., HAUCHECORNE, A. & CHANIN, M. L. - 1991 - Semidiurnal and diurnal tidal effects in the middle Atmosphere as seen by Rayleigh lidar. J. Geophys. Res., **96**:7579-7587.

HAUCHECORNE, A. & CHANIN, M. L. - 1980 - Density and temperature profiles obtained by lidar between 35 and 75 Km. Geophys. Res. Lett., **7**:565-568.

HAUCHECORNE, A. & CHANIN, M. L. - 1982 - A mid-latitude ground-based lidar study of stratospheric warmings and planetary wave propagation. J. Atmos. Terr. Phys., **44**: 577-583.

HAUCHECORNE, A. & CHANIN, M. L. - 1983 - Mid-Latitude Lidar observations of planetary waves in the middle atmosphere during the winter of 1981-1982. J. Geophys. Res., **88**:3843-3849.

HAUCHECORNE, A., BLIX, T., GERNDT, R., KORIN, G. A., MEYER W. & SHEFOV, N. N. - 1987 - Large scale coherence of the mesospheric and upper stratospheric temperature fluctuations. J. Atmos. Terr. Phys., **49**:649-654.

HEDIN, A. E. - 1991 - Extension of the MSIS thermospheric model into the middle and lower atmosphere. J. Geophys. Res., **96**:1159-1172.

JENKINS, D. B., WAREING, D. P., THOMAS L. & VAUGHAN, G. - 1987 - Upper stratospheric and mesospheric temperatures derived from lidar observations at Aberystwyth. J. Atmos. Terr. Phys., **49**: 287-297.

KECKHUT, PH., HAUCHECORNE, A. & CHANIN, M. L. - 1994 - An Anomaly in the temperature climatology seen by Rayleigh lidar: a possible effect of MT Pinatubo eruption. 30th COSPAR Scientific Assembly, Hamburg, Germany, 11-21 july.

KENT, G. S. & WRIGHT, R. W. H. - 1970 - A review of laser radar measurements of atmospheric properties. J. Atmos. Terr. Phys., **32**: 917-943.

KENT, G. S., KEENLISIDE, W., SANDFORD, M. C. W & WRIGHT, R. W. - 1972 - Laser radar observations of atmospheric tides in the 70-100 km height region. J. Atmos. Terr. Phys., **34**: 373-386.

KENT, G. S., CLEMESHA, B. R. & WRIGHT, R. W. - 1967 - High altitude atmospheric scattering of light from laser beam. J. Atmos. Terr. Phys., **29**: 169-181.

McCORMICK, M. P., & VEIGA, R. E. - 1992 - SAGEII measurements of early Pinatubo aerosols. Geophys. Res. Lett., **19**: 155-158.

SHIBATA, T., KOBUCHI, M. & MAEDA, M. - 1986 - Measurements of density and temperature profiles in the middle atmosphere with a XeF lidar. Appl. Optics., **25**: 685-688.

SIMONICH, D. M., CLEMESHA, B. R. & KIRCHHOFF, V. W. J. H. - 1979 - The mesospheric sodium layer at 23° S: Nocturnal and seasonal variations. J. Geophys. Res., **84**: 1543-1549.

Submetido em: 13/06/94
Revisado pelo(s) autor(es) em: 22/09/94
Aceito em: 26/09/94